Cellular Physiology and Biochemistry

Cell Physiol Biochem 2018;48:1563-1578
DOI: 10.1159/000492279
Published online: August 1, 2018
Accepted: June July 22, 2018

Original Paper

Long Non-Coding RNA LINC01260 Inhibits the Proliferation, Migration and Invasion of Spinal Cord Glioma Cells by Targeting CARD11 Via the NF-κB Signaling Pathway

Dong-Mei Wu[a,b] Xin-Rui Han[a,b] Xin Wen[a,b] Shan Wang[a,b] Yong-Jian Wang[a,b] Min Shen[a,b] Shao-Hua Fan[a,b] Juan Zhuang[a,b,c,d] Zi-Feng Zhang[a,b] Qun Shan[a,b] Meng-Qiu Li[a,b] Bin Hu[a,b] Chun-Hui Sun[a,b] Jun Lu[a,b] Yuan-Lin Zheng[a,b]

[a]Key Laboratory for Biotechnology on Medicinal Plants of Jiangsu Province, School of Life Science, Jiangsu Normal University, Xuzhou, [b]College of Health Sciences, Jiangsu Normal University, Xuzhou, [c]School of Environment Science and Spatial Informatics, China University of Mining and Technology, Xuzhou, [d]Jiangsu Key Laboratory for Eco-Agricultural Biotechnology around Hongze Lake, School of Life Sciences, Huaiyin Normal University, Huaian, China

Key Words
Long non-coding RNA LINC01260 • Spinal cord glioma • CARD11 • Nuclear factor-kappa B signaling pathway • Proliferation • Migration • Invasion

Abstract
Background/Aims: Spinal cord glioma is a highly aggressive malignancy that commonly results in high mortality due to metastasis, high recurrence and limited treatment regimens. This study aims to elucidate the effects of long non-coding RNA LINC01260 (LINC01260) on the proliferation, migration and invasion of spinal cord glioma cells by targeting Caspase recruitment domain family, member 11 (CARD11) via nuclear factor kappa B (NF-κB) signaling. ***Methods:*** The Multi Experiment Matrix (MEM) website was used for target gene prediction, and the DAVID database was used for analysis of the relationship between CARD11 and the NF-κB pathway. In total, 60 cases of glioma tissues and adjacent normal tissues were collected. Human U251 glioma cells were grouped into blank, negative control (NC), LINC01260 vector, CARD11 vector, siRNA-LINC01260, siRNA-CARD11, LINC01260 vector + CARD11 vector and LINC01260 + siRNA-CARD11 groups. A dual-luciferase reporter assay was conducted to verify the target relationship between LINC01260 and CARD11. Reverse transcription quantitative polymerase chain reaction (RT-qPCR) and western blot analysis were employed to assess expression of LINC01260, E-cadherin, p53, CARD11, Ki67, N-cadherin, matrix metalloproteinase (MMP)-9, NF-κBp65 and NF-κBp50. MTT, flow cytometry, wound-healing and Transwell assays were performed to examine cell viability, the cell cycle, apoptosis, invasion and migration. Tumor growth was assessed through xenografts in nude mice. ***Results:*** CARD11 was confirmed to be a target gene of LINC01260 and was found to be involved in regulating the NF-κB

D. M. Wu, X.-R. Han and X. Wen contributed equally to this work.

Dr. Jun Lu
and Yuan-Lin Zheng

Key Lab. for Biotech. on Med. Plants of Jiangsu Prov., School of Life Science; School of Health Sciences, Jiangsu Normal Univ.; No. 101, Shanghai Road, Tongshan District, Xuzhou 221116, Jiangsu Province (China) Tel. +86- 0516-83500348, E-Mail lu-jun75@163.com, ylzheng@jsnu.edu.cn

pathway. Compared with adjacent normal tissues, glioma tissues showed reduced expression of LINC01260 and elevated expression of CARD11 and genes related to apoptosis, invasion and migration; activation of NF-κB signaling was also observed. In contrast to the blank and NC groups, an elevated number of cells arrested in G1 phase, increased apoptosis and reduced cell proliferation, invasion and number of cells arrested in S and G2 phases, as well as tumor growth were found for the LINC01260 vector and siRNA-CARD11 groups. ***Conclusions:*** Our findings demonstrate that overexpression of LINC01260 inhibits spinal cord glioma cell proliferation, migration and invasion by targeting CARD11 via NF-κB signaling suppression.

Introduction

Glioma, one of the most common types of primary brain tumors among adults, represents one of the most lethal and aggressive cancers [1]. Multiple chromosomal and genetic abnormalities are associated with glioma, resulting in highly aggressive tumors that will rapidly infiltrate, invade and destroy neighboring tissue, particularly in the spinal cord [2]. Low-grade gliomas are often associated with neurological disability [3]. Due to the high recurrence rate, infiltrative nature and limited treatment options, the prognosis of high-grade glioma remains poor [4]. Despite many advances in medical and surgical therapy in recent years, glioma remains a fatal disease, with overall poor survival [5]. Moreover, radiotherapy treatment for spinal cord glioma is associated with worsened outcomes [6]. Interestingly, one study provides new insight for understanding the function of the long non-coding RNA taurine up-regulated gene 1 (lncRNA TUG1) in cancer biology, with the potential of TUG1 overexpression in glioma therapy [7].

As a relatively new class of non-coding RNAs, lncRNAs have been widely reported to function in different biological processes because of their role in gene expression [8]. Certain lncRNAs can regulate the effects of transcription factors by serving as co-regulators and may be involved in epigenetic regulation, including X-chromosome inactivation, and in chromatin and histone modification [9]. Furthermore, emerging evidence has revealed that lncRNAs have a close relationship with diverse malignancies and may act as tumor suppressors in different tumor types [10]. Caspase recruitment domain family, member 11 (CARD11), a scaffold protein that forms a complex with B cell lymphoma-10 and mucosa-associated lymphoid tissue (MALT1), is required for antigen receptor-triggered nuclear factor kappa B (NF-κB) activation in both B- and T-cells [11]. NF-κB transcription factors are often evolutionarily conserved, possibly coordinating regulators of inflammatory and immune responses and playing a pivotal role in metabolic and oncogenesis disorders [12]. For example, NF-κB signaling orchestrates several pivotal biological processes in cancer development and progression by inducting transcription of various target genes controlling the cell cycle, apoptosis, and invasion [13-15]. Importantly, LINC01260 is down-regulated in spinal cord glioma (GEO database GSE15824) and is co-expressed with CARD11 in various cancers, including skin cutaneous melanoma, liver hepatocellular carcinoma, kidney clear cell carcinoma, breast invasive carcinoma, brain lower grade glioma, prostate adenocarcinoma and glioblastoma multiforme [16]. Nonetheless, how LINC01260 targets CARD11 in spinal cord glioma remains unclear. This study was performed to explore the role of LINC01260 in the proliferation, migration and invasion of spinal cord glioma cells by targeting CARD11 via the NF-κB pathway.

Materials and Methods

Target gene prediction

The Multi Experiment Matrix (MEM, http://biit.cs.ut.ee/mem/) website was used for target gene prediction for LINC01260. MEM is a web-based tool for conducting co-expression queries among a large number of collections of gene expression experiments. MEM can provide access to hundreds of publicly

available gene expression datasets of various tissues, diseases and conditions and is managed by both species and microarray platform types [17]. The specific approaches are shown at https://biit.cs.ut.ee/beta_mem/help/mem_ismb_2009.pdf. In addition, the DAVID website (http://david.ncifcrf.gov/) was adopted for Kyoto Encyclopedia of Genes and Genomes (KEGG) pathway enrichment analysis to confirm the main biochemical metabolic and signaling pathways related to the obtained target genes.

Sample collection

Following verification of spinal cord glioma by pathological examination, 60 cases of spinal cord glioma and adjacent normal tissues were obtained after surgery from patients at Key Laboratory for Biotechnology on Medicinal Plants of Jiangsu Province, School of Life Science, Jiangsu Normal University between 2007 and 2011. Among the patients, 34 were male and 26 female, with age range from 3 to 82 years. Prior to surgery, none of the patients had any distant spinal metastasis or was treated with other regimens. After collection of spinal cord glioma and adjacent tissues (2 cm on the verge) during surgery, a portion of the fresh samples were fixed in 10% formaldehyde solution (UFML04360, Shanghai JunruiBiotch Company, Shanghai, China) after extraction, and the remainder was preserved at -80°C for further experiments. All sample collections were approved by the patients via informed consent and were in accordance with the requirements of the Ethics Committee of Key Laboratory for Biotechnology on Medicinal Plants of Jiangsu Province, School of Life Science, Jiangsu Normal University.

Immunohistochemistry

All tissue sections were placed in an incubator at 60°C for 1 h, dewaxed with xylene, dehydrated by a graded alcohol series and incubated in 3% H_2O_2 (BD5024, Bioworld Technology Inc, Minneapolis, Minnesota, USA) at 37°C for 30 min. The sections were then washed4 times with phosphate-buffered saline (PBS) (2 min each time), and antigen retrieval was performed using the high-pressure method for 2 min. Next, the sections were placed in 0.01 M citric acid buffer (pH 6.0) and heated at 95°C for 20 min followed by immersion in 3% H_2O_2 for 15 min to block exogenous peroxidase activity. The sections were blocked with normal goat serum working fluid (Ns01-01, Bai Taike Biotechnology Co., Ltd., Henan, China) at 37°C for 10 min. The diluted primary antibody, rabbit anti-human polyclonal antibody CARD11 (1: 500, bs-6201R, Bioss, Beijing, China), was added and incubated at 4°C overnight, followed by washing three times with PBS for 3 min. Next, the horseradish peroxidase (HRP)-labeled goat anti-rabbit secondary antibody working solution was added (1: 1000, A21020, Abbkine, California, San Francisco, CA, USA) and incubated at room temperature for 30 min, after which the sections were stained with diaminobenzidine (DAB) (3, 3-diaminobenzidine, AR1000, Wuhan Bude Biological Engineering Co., Ltd. Hubei, China). The sections were rinsed remove excess dye, and mounted. PBS, instead of the primary antibody, was used as a negative control (NC), and known positive sections were used as positive controls. Color development was observed under a microscope, with the cell membrane or cytoplasm of positively staining cells showing a tan color. Section images were captured under the microscope, and five randomly selected high-magnification fields with 100 cells were counted.. The average percentage of positive cells in each section was regarded as the positivity rate.

RNA isolation and quantitation

Total RNA was extracted from the spinal cord glioma and adjacent normal tissues preserved at -80°C according to the instructions of an miRNeasy Mini Kit (217004, Qiagen, Hilden, Germany); $(A)_{260}/A_{230}$ and A_{260}/A_{280} ratios were evaluated using a Nanodrop 2000 micro-ultraviolet spectrophotometer (1011U, NanoDrop Technologies Inc., Wilmington, USA) for determination of the concentration and purity of the extracted total RNA. The obtained RNA was then reverse transcribed into cDNA according to the instructions of TaqMan MicroRNA Assays Reverse Transcription Primer (4427975, Applied Biosystems Inc. Carlsbad, CA, USA). The reaction conditions were 37°C for 30 min and 85°C for 5 s. The obtained cDNA was diluted to 50 ng/μl, and 2 μl was used for amplification in a 25-μl volume. Primers designed to amplify LINC01260, CARD11, Ki67, N-cadherin, E-cadherin, matrix metalloproteinase (MMP)-9, p53, NF-κBp50 and NF-κBp65 were synthesized by TaKaRa (Takara Biotechnology Ltd., Liaoning, China) (Table 1). Reverse transcription quantitative polymerase chain reaction (RT-qPCR) was conducted using the ABI7500 quantitative PCR instrument (7500, ABI Company, Oyster Bay, NY, USA), with the following conditions: pre-denaturation at 95°C for 10 min and 40 cycles of denaturation at 95°C for 10 s, annealing at 60°C for 20 s, and extension at 72°C for 34 s. The fluorescence quantitative PCR 20-μl reaction mixture consisted of 10 μl of SYBR Premix

Ex TaqTM II, 0.8 μl of PCR Forward Primer (10 μM), 0.8 μl of PCR Reverse Primer (10 μM), 0.4 μl of ROX Reference Dye, 2.0 μl of cDNA template, and 6.0 μl of sterile distilled water. U6 was used as the internal reference for LINC01260, and β-actin was used for CARD11, Ki67, N-cadherin, E-cadherin, MMP-9, p53, NF-κBp50 and NF-κBp65. The $2^{-\Delta\Delta Ct}$ value represents the relationship of target gene expression between experimental and control groups. The formula was as follows: $\Delta\Delta CT = \Delta Ct_{\text{experiment group}} - \Delta Ct_{\text{control group}}$, and $\Delta Ct = Ct_{\text{miRNA}} - Ct_{\beta\text{-actin}}$. Each group of experiments was repeated 3 times (mRNA expression was detected after 48 h of transfection, and the experimental methods were the same as those presented above).

Table 1. Primer sequences for RT-qPCR. Note: MMP, matrix metalloproteinase; LINC01260, non-coding RNA LINC01260; CARD11, caspase recruitment domain family, member 11; NF-κB, nuclear factor-kappa B; F, forward; R, reverse; RT-qPCR, reverse transcription quantitative polymerase chain reaction

Gene	Primer sequence
LINC01260	F: 5'-CCACACACACCAGAGAGGAC-3'
	R: 5'-ATTATCCACACAGCACGCCA-3'
CARD11	F: 5'-GTGCCCCCTCTCCACAGT-3'
	R: 5'-AGTACCGCTCCTGGAAGGTT-3'
Ki67	F: 5'-GCCCCAACCAAAAGAAAGTCT-3'
	R: 5'-CATCAAGGAACAGCCTCAACCATCAGGA-3'
E-cadherin	F: 5'-CGCATTGCCACATACACTCT-3'
	R: 5'-TTGGCTGAGGATGGTGTAAG-3'
N-cadherin	F: 5'-AGTCAACTGCAACCGTGTGT-3'
	R: 5'-AGCGTTCCTGTTCCACTCAT-3'
MMP-9	F: 5'-TTCCCTGGAGACCTGAGAACC-3'
	R: 5'-CGACACCAAACTGGATGACGC-3'
p53	F: 5'-ACATCTGGCCTTGAAACCAC-3'
	R: 5'-CGAGACCCAGTCTCAAAGAA-3'
NF-κBp50	F: 5'-AACGCATCCCAAGGTGCTGGAA-3′
	R: 5'-GCAGCTGGAAAAGCTCAAGCCA-3′
NF-κBp65	F: 5'-TTCCCTGAAGTGGAGCTAGGA-3′
	R: 5'-CATGTCGAGGAAGACACTGGA-3′
U6	F: 5'-GCTTCGGCAGCACATATACTAAAAT-3′
	R: 5'-CGCTTCACGAATTTGCGTGTCAT-3′
β-actin	F: 5”-ATAGCACAGCCTGGATAGCAACGTAC-3'
	R: 5'-CACCTTCTACAATGAGCTGCGTGTG-3'

Western blot analysis

The spinal cord glioma and adjacent normal tissues preserved at -80°C were placed in a glass grinder with 1 ml of tissue lysis buffer (BB-3209, Beibo Biology, Shanghai, China) for homogenization at 3000 r/min until fully dissociated. The tissues were then placed in an ice bath for 30 min, with shaking once every 10 min, and centrifuged (12000 r/min) for 20 min at 4°C; the lipid layer discarded. The liquid supernatant was collected for protein concentration detection using a bicinchoninic acid (BCA) kit (20201ES76, Yeasen Inc, Shanghai, China); deionized water was used for adjusting the protein content to 30 μg of protein/lane. Each group of samples was mixed with the corresponding amount of 5 × sodium dodecyl sulfate (SDS) loading buffer, boiled at 100°C for 5 min, cooled on ice and centrifuged. The proteins were separated by 10% SDS-polyacrylamide gel electrophoresis (PAGE), with a 5% stacking gel, and transferred to nitrocellulose membranes. The membranes were blocked overnight with 5% skim milk powder at 4°C. Diluted (1: 500) primary rabbit anti-human polyclonal antibodies, including anti-CARD11 (bs-6201R), -Ki67 (bs-5570R), -N-cadherin (bs-1172R), E-cadherin (bs-10009R), MMP-9 (bs-4593R), NF-κBp65 (bs-0465R) and NF-κBp50 (bs-1194R) (all antibodies were purchased from Beijing Boao Sen Biotechnology Co., Ltd., Beijing, China), and diluted rabbit anti-rat polyclonal p53 (1: 1000, ABP50382, Abbkine, California, USA) and anti-β-actin (ABP57456, Abbkine, California, USA) antibodies were added and incubated overnight. The membrane was then washed 3 times with PBS at room temperature (5 min/time), and the diluted HRP-labeled IgG goat anti-rabbit secondary antibody (1: 10000, A21020, Abbkine, California, USA) was added for l h at 37°C, after which the membrane was washed3 times with PBS at room temperature (5 min/time). The membrane was incubated with enhanced chemiluminescence (ECL) solution (ECL808-25, Biomiga, San Diego, CA, USA) at room temperature for 1 min. The liquid was then removed, and the membrane was covered with preservative film and exposed to X-ray film (36209ES01, Qianchen Biological Technology Co., Ltd., Shanghai, China). The ratio between the gray value of the target band and the internal reference band was used as the relative expression level of the protein, with β-actin as an internal reference. Each group of experiments was repeated 3 times; cells were examined after transfection for 72 h.

Cell culture

The human glioma cell line U251 (PT-1903, ATCC, Rockefeller, Maryland, USA) was seeded in Dulbecco's modified Eagle medium (DMEM) (GNM-12800, Shanghai Chemical Science and Technology Co., Ltd., Shanghai, China) containing 10% fetal bovine serum (FBS) and incubated in a 5% CO_2 incubator with saturated humidity at 37°C. The cells were subcultured once every 2 - 3 d, and cells in logarithmic growth phase were collected for use.

Construction of overexpression and RNA interference expression vectors

Based on the known transcript sequences of the LINC01260 and CARD11 genes in GenBank, the full-length sequences of LINC01260, CARD11 and small inhibitory (siRNA; 3 pairs of siRNA sequences were designed for each gene), as well as negative control (NC) sequences, were designed online using the Ambion website and were synthesized by Shanghai Ji Kai Gene Biology Co., Ltd. (Shanghai, China). The correct sequence was cloned into the vector pcDNA3.1 (VPI0001, Invitrogen Inc., Carlsbad, CA, USA) at Hind III and XHo I restriction sites and ligated at 16ºC for 1 h. The ligation product was added to competent *Escherichia coli* DH5α cells (D9052, Takara Biotechnology Ltd., Liaoning, China). Resistant colonies were screened and identified by colony PCR, and positive clones were sequenced. The plasmid was stored at -20°C.

Cell transfection and grouping

U251 glioma cells in logarithmic growth phase were digested with 0.25% trypsin (25200056, Gibco, Grand Island, NY, USA), re-suspended in serum M199 medium containing 10% FBS to a concentration of 1×10^5 cells/ml, and inoculated in a 6-well culture plate. When confluence reached 80%, transfection was conducted. Next, 200 µl of serum-free Opti-MEM medium (31985, Gibco, Grand Island, NY, USA) was used to dilute 6 µl of Lipofectamine 2000 (11668-019, Invitrogen Inc., Carlsbad, CA, USA) and 2 µg of the target plasmid respectively, followed by even mixing and incubation at room temperature for 10 min. The two solutions were subsequently mixed and incubated at room temperature for 20 min. The medium in the 6-well plate was discarded, and 180 µl of Opti-MEM medium was added to each well, followed by addition of the transfection mixture and incubation at 37°C in a 5% CO_2 incubator for 18 h. Next, new medium (INV-00002, INNOVATE, Jiangsu, China) was added for further incubation for 24 h. The cells were collected for subsequent experiments. The cells were divided into the blank group (no transfection), NC group (transfected with the LINC01260 NC sequence), LINC01260 vector group (transfected with the LINC01260 overexpression plasmid), CARD11 vector group (transfected with the CARD11 overexpression plasmid), siRNA-LINC01260 group (transfected with the LINC01260 siRNA-CARD1 plasmid), siRNA-CARD11 group (transfected with the siRNA--CARD1 plasmid), LINC01260 vector + CARD11 vector group (transfected with LINC01260 and CARD11 overexpression plasmids) and siRNA-LINC01260 + siRNA-CARD11 group (co-transfected with LINC01260 and siRNA-CARD1 plasmids).

Dual-luciferase reporter assay

The bioinformatics prediction website lncRNA Targets (http://www.herbbol.org:8001/lrt/) was employed to analyze LINC01260 target genes using lncRNA (query sequences) and RNA (subjects) sequences. All of the results were presented in a table with green and red colors based on the ΔG/n threshold value, the cutoff value. Good stability of internal base pairs for two sequences reflects the relatively stable combination between the query and subject [18]. HEK-293T (AT-1592, ATCC, Manassas, VA, USA) cells were seeded in a 24-well plate and cultured for 24 h. A CARD11 dual-luciferase reporter gene plasmid (pmiRRB-CARD11-3'UTR) was constructed and co-transfected with the LINC01260, siRNA-LINC01260 or NC plasmid into HEK-293T cells. Following transfection for 48 h, the medium was discarded, and the cells were washed twice with PBS, collected and lysed. Luciferase activity was measured using a dual-luciferase reporter assay system (Dual-Luciferase® Reporter Assay System, E1910, Promega Corporation, Madison, WI, USA). Firefly luciferase activity was measured by adding 50 µl of firefly luciferase solution for every 10 µl of the cell sample; 50 µl of Renilla luciferase was also added. The ratio of luciferase activity to Renilla activity was regarded as the relative luciferase activity. The experiment was repeated three times.

The 3-(4, 5-dimethylthiazol-2-yl)-2, 5-diphenyltetrazolium bromide (MTT) assay

Following transfection for 24 h, cells were collected, washed twice with PBS and digested with 0.25% trypsin to prepare a single-cell suspension. Following cell counting, 3×10^4 - 5×10^4 cells were inoculated per well (0.1 ml) into a 96-well plate, with 6 duplicate wells for each plate. The cells were then placed in an incubator, and cell adhesion was examined at 0 h, 24 h, 48 h and 72 h. Then, 20 µl of 0.5% MTT solution (M2128, Sigma-Aldrich Chemical Company, St Louis MO, USA) was added to each well, and the samples were cultured for another 4 h, after which the supernatant was removed. After this step, 100 µl of dimethyl sulfoxide (DMSO, D5879-100ML, Sigma-Aldrich Chemical Company, St Louis MO, USA) was added to each well, and the plate was slightly shaken for 10 min to completely dissolve the formazan crystals produced by living cells. A microplate reader (BS-1101, DetieExperimental Equipment Co., Ltd., Nanjing, Jiangsu, China)

was used to detect the optical density (OD) value for each well at 492 nm. Each experiment was repeated three times, and a cell viability curve was drawn with the time point as the abscissa and the OD value as the ordinate.

Flow cytometry

Propidium iodide (PI) single staining: following transfection for 24 h, cells were collected, digested with 0.25% trypsin, and centrifuged (1000 r/min) for 5 min; the pellet was washed three times with cold PBS. The cells were then re-suspended in PBS at a concentration of 1×10^5 cells/ml and fixed with 2 ml of -20°C pre-cooled 75% ethanol alcohol at 4ºC for 30 min. Following this step, the cells were centrifuged, and the ethanol removed; the samples were washed twice with PBS. Next, 100 µl of RNase A was added, and the samples were protected from light in a 37°C water bath for 30 min; 400 µl of PI dye (P4170, Sigma-Aldrich Chemical Company, St Louis MO, USA) was added and mixed at 4°C for 30 min, away from light. Flow cytometry (CA 92821, CytoFLEX, Beckman Coulter Life Sciences, Brea, CA, USA) was performed to record red fluorescence for detection of the cell cycle at an excitation wavelength of 488 nm. The experiment was repeated three times.

Annexin-V/PI double labeling method: following transfection for 48 h, cells were digested with 0.25% trypsin (PYG0107, Wuhan Boster Biological Technology Co., LTD., Hubei, China) without ethylene diamine tetraacetic acid (EDTA), collected in a flow cytometry tube, and centrifuged; the supernatant was discarded. The cells were then washed three times in cold PBS and centrifuged again, with the supernatant discarded. According to the instructions of Annexin-V-FITC Apoptosis Detection Kit (K201-100, Biovision, CA, USA), the Annexin-V-FITC dye was prepared with Annexin-V-FITC, PI, 4-(2-hydroxyethyl)-1-piperazinethane sulfonic acid (HEPES) buffer at a ratio of 1: 2: 50. Each 100 µl of dye solution was used to resuspended 1×10^6 cells. The samples were shaken and mixed. Following incubation at room temperature for 15 min, 1 ml of HEPES buffer solution was added. FITC and PI fluorescence was detected using 615-nm and 690-nm bandpass filters at a wavelength of 488 nm, and apoptosis was assessed (the experiment was repeated 3 times). The flow cytometry scatter diagram shows that the right lower quadrant contained early apoptotic cells, the upper right quadrant contained necrotic and apoptotic cells, the upper left quadrant contained mechanically injured cells or necrotic cells, and the left lower quadrant contained living cells. Apoptosis rate (%) = percentage of early apoptosis + percentage of late apoptosis. The experiment was repeated three times.

Wound-healing assay

Following transfection for 48 h, cells were digested at a density of 5×10^5 cells/ml; 100 µl of the cell suspension was seeded in a 24-well plate and cultured at 37°C in 5% CO_2 to form a cell monolayer. The cells were then scratched and washed with PBS. The medium was replaced with one (RPMI 1640, 350-030-CL, Wisent Biological Technology Co., Ltd., Jiangsu, China) containing 10 g/L bovine serum albumin (BSA) (9998S, Shanghai Beinuo Biological Technology Co., Ltd., Shanghai, China) and 1% FBS. The migration distance was measured under a microscope. Following 24 h of culture, the medium was replaced by fresh medium (RPMI 1640) supplemented with 10% FBS for 24 h. The relative distance of cell migration towards the injured area was measured under a microscope. The experiment was repeated three times.

Transwell assay

Following 48 h of transfection, cells were starved in serum-free medium for 24 h, digested with trypsin, and washed twice with PBS. Serum-free Opti-MEMI medium containing 10 g/L bovine serum albumin (BSA; 9998S, Shanghai Beinuo Biotechnology Co., Ltd., Shanghai, China) was used to re-suspend the cells at the density of 5×10^5 cells/ml. Experiments were performed using a 24-well plate and an 8-µm Transwell chamber (3422, Beijing You Nikon Biotechnology Co., Ltd., Beijing, China), with 3 chambers for each group, and 100 µl of cell suspension was added per well. A total of 600 µl of 10% RPMI 1640 medium (350-030-CL, Visent Biotechnology Co., Ltd., Jiangsu, China) was added to the lower chamber, and the plates were placed in a 5% CO_2 incubator at 37°C. For the migration test, the cells were fixed after 48 h with 4% paraformaldehyde for 30 min and subsequently placed in 0.2% Triton X-100 (HFH10, Invitrogen Inc., Carlsbad, CA, USA) solution for 15 min; the cells were then stained with 0.05% crystal violet (71019944, Shanghai Rongbai Biotechnology Co., Ltd., Shanghai, China) for 5 min. For the invasion test, 50 µl of Matrigel matrix gel (YB356234, Shanghai Yubo Biotechnology Co., Ltd., Shanghai, China) was added to cover the

chamber before the experiment. After 48 h, the above method of fixing and staining was applied. The number of stained cells was counted under an inverted microscope. Five fields were randomly selected to count the cell number, and the result was expressed as a mean value. The experiment was repeated three times.

Xenograft tumors in nude mice

BALB/c nude mice aged approximately 4 weeks were purchased from the Experimental Animal Center of the Third Military Medical University (Chongqing, China). All mice were housed in laminar flow cabinets under specific pathogen-free (SPF) conditions with a constant temperature (24°C - 26°C) and humidity (45% - 55%). Forage and drinking water were given to mice after high-temperature disinfection. Then the mice were allocated into blank, NC, LINC01260 vector, CARD11 vector, siRNA-LINC01260, siRNA-CARD11, LINC01260 vector + CARD11 vector and siRNA-LINC01260 + siRNA-CARD11 groups (5 mice in each group). Following transfection of U251 glioma cells, the subcutaneous part of the nude mice was injected with 200 μl of a U251 cell suspension containing 1×10^6 cells for each group. The maximum diameter (a) and minimum diameter (b) of the tumors that appeared were measured using a Vernier caliper. Tumor volume was calculated according to the formula $V = a \times b^2 \times 0.5$ [19], with an interval of 5 d, 4 times each. Later, tumor growth curves were drawn. The mice were killed using the cervical dislocation method. This study was carried out in strict accordance with the recommendations in the Guide for the Care and Use of Laboratory Animals of the National Institutes of Health.

Statistical analysis

The data were processed with the SPSS 21.0 statistical package (IBM, Armonk, NY, USA). Measurement data were normally distributed, and the results are expressed as the mean ± standard deviation. Comparison between expression of different factors in cancer tissues and adjacent normal tissues was performed using the *t*-test. Comparisons among multiple groups were achieved using one-way analysis of variance (ANOVA), and those between two groups were performed by the least significant difference (LSD) test. In addition, repeated measures ANOVA was employed to assess the results of the MTT assay and tumor growth curves, and the chi-square test was used for comparisons of CARD11 protein expression between groups. A significant difference was considered at $p < 0.05$.

Results

CARD11 is predicted as a target gene of LINC01260

According to the MEM website, CARD11 was predicted as a target gene of LINC01260 (Table 2). Its participation in the NF-κB signaling pathway (Fig 1) suggested that CARD11 is a target gene of LINC01260.

Higher rate of CARD11 expression is found in glioma tissues

Immunohistochemistry was employed to determine CARD11 protein expression. The CARD11 protein was primarily found in the cytoplasm, with a small amount in the plasma membrane. Positive cells stained brown or tan. Compared with adjacent normal tissues [56.7% (34/60)], the rate of CARD11 protein expression was clearly increased in glioma tissues [21.7% (13/60)] ($p < 0.05$) (Fig 2). Based on these findings, CARD11 is expressed at a higher level in glioma tissues.

LINC01260, E-cadherin and p53 are expressed at low levels and CARD11, Ki67, N-cadherin, MMP-9, NF-κBp65 and NF-κBp50 at high levels in glioma tissues

RT-qPCR and western blot analyses were conducted to determine expression of LINC01260, E-cadherin, p53, CARD11, Ki67, N-cadherin, MMP-9, NF-κBp65 and NF-κBp50. Compared with adjacent normal tissues, LINC01260 expression was decreased 0.69-fold, and mRNA and protein expression of E-cadherin was reduced 0.4-fold and 0.41-fold, respectively. Furthermore, p53 (mRNA 0.35-fold; protein 0.47-fold) was decreased substantially ($p < 0.05$). In contrast, expression of CARD11 (mRNA 2.22-fold; protein 1.89-fold), Ki67 (mRNA 1.91-fold; protein 2.93-fold), N-cadherin (mRNA 2.04-fold; protein 1.57-fold), MMP-9 (mRNA 1.89-fold; protein 2.05-fold), NF-κBp65 (mRNA 2.05-fold; protein 2.36-fold) and

NF-κBp50 (mRNA 1.89-fold; protein 2.58-fold) were markedly increased in glioma tissues ($p < 0.05$) (Fig 3). These results provide evidence that LINC01260, E-cadherin and p53 are expressed at low levels and that CARD11, Ki67, N-cadherin, MMP-9, NF-κBp65 and NF-κBp50 are expressed at high levels in glioma tissues.

LINC01260 inhibits CARD11 activity

Dual-luciferase reporter gene assays and bioinformatics prediction were applied to analyze the relationship between LINC01260 and CARD11. Based on bioinformatics prediction, the binding site for LINC01260 and CARD11 were present in the CARD11 3' untranslated region (UTR), with a free energy between of ΔG = -76.38 and ΔG/n = -0.066. Therefore, CARD11 was confirmed as a target gene for LINC01260. Compared with the NC group, relative luciferase activity was significantly decreased in the LINC01260 vector group and significantly increased in the siRNA-LINC01260 group ($p < 0.05$), indicating that LINC01260 can target CARD11 and may inhibit CARD11 activity (Fig 4).

LINC01260 represses CARD11 expression and inactivates the NF-κB pathway

RT-qPCR and western blot analyses were conducted to assess expression of LINC01260,

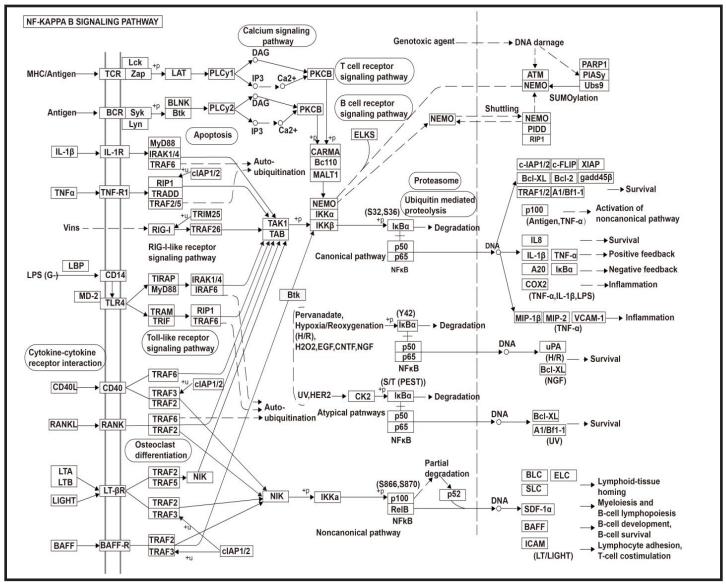

Fig. 1. CARD11 is involved in the NF-κB signaling pathway.Notes: CARD11, caspase recruitment domain family, member 11; NF-κB, nuclear factor-kappa B.

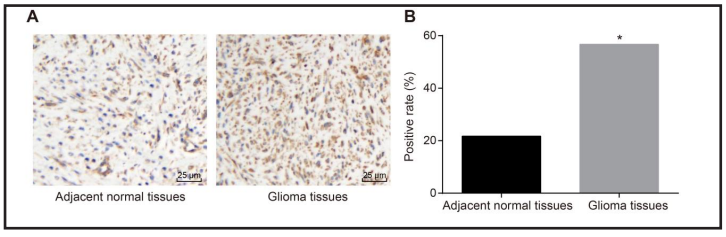

Fig. 2. Positive expression of the CARD11 protein in glioma tissues and adjacent normal tissues, as determined by immunohistochemistry. Notes: A, Immunohistochemistry image of CARD11 expression in glioma tissues and adjacent normal tissues (400 ×). B, Histogram of comparisons of CARD11 expression rates between glioma tissues and adjacent normal tissues; *, p<0.05, compared with adjacent normal tissues (n = 60). CARD11, caspase recruitment domain family, member 11.

Table 2. KEGG pathway enrichment analysis for target genes of LINC01260. Note: LINC01260, non-coding RNA LINC01260;NF-kB, nuclear factor-kappa B; KEGG, Kyoto Encyclopedia of Genes and Genomes

Pathway	p value	Gene
Primary immunodeficiency-related pathway	1.27754473666641E-11	ADA;ICOS;IL2RG;LCK;RFX5;ZAP70;CD3D;CD3E;CD8A;CD8B
Hematopoietic cell lineage- pathway	1.4167798045861E-09	CR2;CD1A;CD1B;CD1E;CD2;CD3D;CD3E;CD3G;CD5;CD7;CD8A;CD8B
Th1 and Th2 cell differentiation- related pathway	0.0000189457355057598	IL2RG;LCK;PLCG1;PRKCQ;ZAP70;CD3D;CD3E;CD3G
Measles-related pathway	0.0000389389132997575	IL2RG;SH2D1A;OAS2;OAS3;PRKCQ;CD3D;CD3E;CD3G;CD28
Th17 cell differentiation	0.0000611634263216754	IL2RG;LCK;PLCG1;PRKCQ;ZAP70;CD3D;CD3E;CD3G
Natural killer cell-mediated cytotoxicity	0.0006940371281835	ICAM2;LCK;LCP2;SH2D1A;PLCG1;VAV1;ZAP70
NF-kB signaling pathway	0.00111694624666703	CARD11
Cell adhesion molecules (CAMs)	0.00185173280840545	ICOS;ICAM2;CD2;CD6;CD8A;CD8B;CD28
Basal cell carcinoma	0.0317702104185145	LEF1;HHIP;TCF7

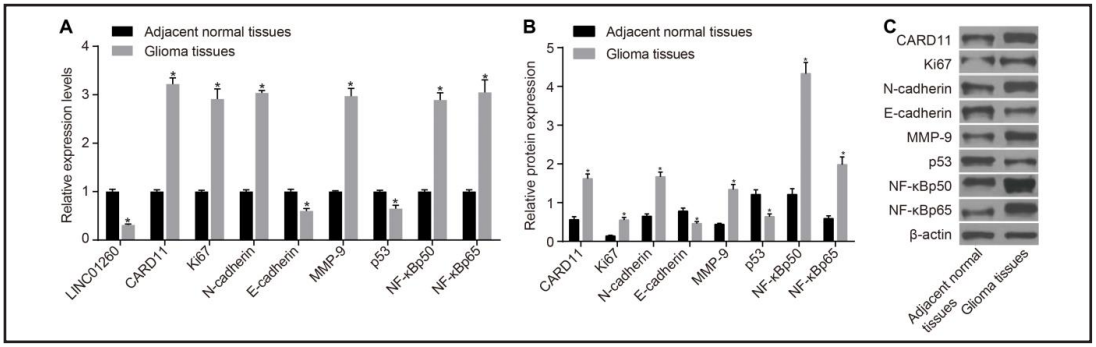

Fig. 3. LINC01260 expression and mRNA and protein expression of E-cadherin, p53, CARD11, Ki67, N-cadherin, MMP-9, NF-κBp65 and NF-κBp50 in glioma tissues and adjacent normal tissues, as identified by RT-qPCR and western blot analyses. Notes: A, LINC01260 expression and mRNA expression of E-cadherin p53, CARD11, Ki67, N-cadherin, MMP-9, NF-κBp65 and NF-κBp50. B, Histogram of protein expression of E-cadherin p53, CARD11, Ki67, N-cadherin, MMP-9, NF-κBp65 and NF-κBp50. C, Western blot analysis results for E-cadherin, p53, CARD11, Ki67, N-cadherin, MMP-9, NF-κBp65 and NF-κBp50; *, $p<0.05$, compared with adjacent normal tissues (n = 60). MMP-9, matrix metalloproteinase-9; LINC01260, non-coding RNA LINC01260; CARD11, caspase recruitment domain family, member 11; NF-κB, nuclear factor-kappa B; RT-qPCR, reverse transcription quantitative polymerase chain reaction.

Fig. 4. CARD11 was confirmed as a target gene for LINC01260 in HEK-293T cells using a dual-luciferase reporter assay. Notes: A, Three binding sites for LINC01260 in the CARD11 3'UTR, as revealed by the online prediction website lncRNA Targets (http://www.herbbol.org:8001/lrt/). B, Luciferase activity determined by a dual-luciferase reporter assay for the relationship between LINC01260 and CARD11; *, $p<0.05$, compared with the NC group (n = 3). NC, negative control; LINC01260, non-coding RNA LINC01260; CARD11, caspase recruitment domain family, member 11.

E-cadherin, p53, CARD11, Ki67, N-cadherin, MMP-9, NF-κBp65 and NF-κBp50. Compared with the blank group, the LINC01260 vector group showed 2.39-fold increases and the LINC01260 vector + CARD11 vector group 1.37-fold increases, demonstrating markedly increased LINC01260 expression ($p < 0.05$). Conversely, the siRNA-LINC01260 (0.74-fold) group and the siRNA-LINC01260 + siRNA-CARD11 (0.68-fold) group exhibited substantially decreased LINC01260 expression ($p < 0.05$). No notable difference in LINC01260 expression was found in the CARD11 vector and siRNA-CARD11 groups ($p > 0.05$). Expression of CARD11 (mRNA 0.65-fold; protein 0.52-fold), Ki67 (mRNA 0.30-fold; protein 0.52-fold), N-cadherin (mRNA 0.64-fold; protein 0.40-fold), MMP-9 (mRNA 0.65-fold; protein 0.58-fold), NF-κBp65 (mRNA 0.65-fold; protein 0.72-fold) and NF-κBp50 (mRNA 0.76-fold; protein 0.58-fold) in the LINC01260 vector group was decreased ($p < 0.05$). In contrast, expression of E-cadherin (mRNA 0.38-fold; protein 0.57-fold) and p53 (mRNA 0.35-fold; protein 0.55-fold) was markedly increased (all $p < 0.05$). The siRNA-CARD11 group presented reduced expression of CARD11 (mRNA 0.65-fold; protein 0.54-fold), Ki67 (mRNA 0.31-fold; protein 0.48-fold), N-cadherin (mRNA 0.66-fold; protein 0.37-fold), MMP-9 (mRNA 0.64-fold; protein 0.59-fold), NF-κBp65 (mRNA 0.67-fold; protein 0.73-fold) and NF-κBp50 (mRNA 0.75-fold; protein 0.57-fold) (all $p < 0.05$) but elevated expression of E-cadherin (mRNA 0.36-fold; protein 0.59-fold) and p53 (mRNA 0.37-fold; protein 0.56-fold) (all $p > 0.05$).

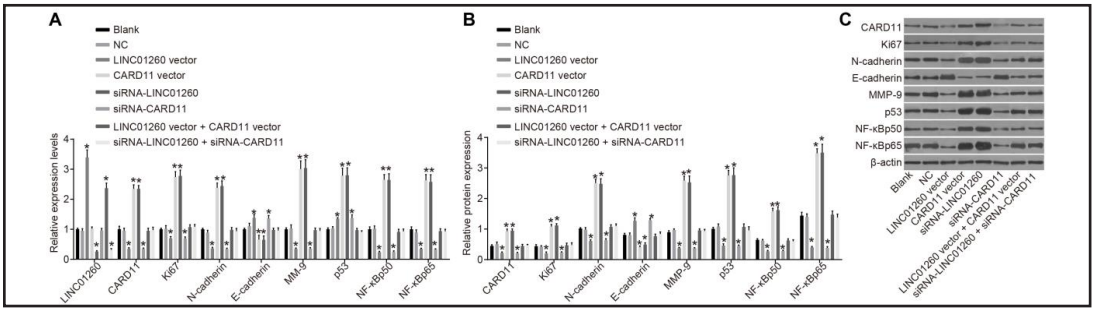

Fig. 5. LINC01260 overexpression reduces the expressions of E-cadherin, p53, CARD11, Ki67, N-cadherin, MMP-9, NF-κBp65 and NF-κBp50 in U251 cells after transfection, as verified by RT-qPCR and western blot analyses. Notes: A, LINC01260 expression and mRNA expressions of E-cadherin, p53, CARD11, Ki67, N-cadherin, MMP-9, NF-κBp65 and NF-κBp50 in U251 cells among eight groups. B, Protein expression of E-cadherin, p53, CARD11, Ki67, N-cadherin, MMP-9, NF-κBp65 and NF-κBp50 among eight groups in U251 cells. C, Western blot analysis results for E-cadherin, p53, CARD11, Ki67, N-cadherin, MMP-9, NF-κBp65 and NF-κBp50 among eight groups in U251 cells; *, p<0.05, compared with blank and NC groups (n = 3). NC, negative control; MMP, matrix metalloproteinase; LINC01260, non-coding RNA LINC01260; CARD11, caspase recruitment domain family, member 11; NF-κB, nuclear factor-kappa B; RT-qPCR, reverse transcription quantitative polymerase chain reaction.

Although the LINC01260 vector and siRNA-CARD11 groups showed no notable differences in mRNA and protein expression of E-cadherin, p53, CARD11, Ki67, N-cadherin, MMP-9, NF-κBp65 and NF-κBp50 (all $p > 0.05$), the CARD11 vector group did exhibit altered expression of CARD11 (mRNA expression increased 1.35-fold; protein expression increased 1.06-fold), Ki67 (mRNA expression increased 1.45-fold; protein expression declined 1.55-fold), N-cadherin (mRNA expression down-regulated 1.38-fold; protein expression increased 1.46-fold), MMP-9 (mRNA expression fell 2.01-fold; protein expression fell 1.88-fold), NF-κBp65 (mRNA expression decreased 1.63-fold; protein expression decreased 1.42-fold) and NF-κBp50 (mRNA expression declined 1.65-fold; protein expression declined 1.43-fold) ($p < 0.05$) as well as elevated expression of E-cadherin (mRNA 1.36-fold; protein 1.24-fold) and p53 (mRNA 1.79-fold; protein 1.73-fold) ($p < 0.05$). In the siRNA-LINC01260 group, up-regulated expression of CARD11 (mRNA 1.35-fold; protein 1.10-fold), Ki67 (mRNA 1.78-fold; protein 1.55-fold), N-cadherin (mRNA 1.44-fold; protein 1.43-fold), MMP-9 (mRNA 2.04-fold; protein 1.81-fold), NF-κBp65 (mRNA 1.5-fold; protein 1.43-fold), NF-κBp50 (mRNA 1.64-fold; protein 1.50-fold) (all $p < 0.05$), E-cadherin (mRNA 1.35-fold; protein 1.21-fold) and p53 (mRNA 1.80-fold; protein 1.74-fold) was observed. However, the data showed no difference between the CARD11 vector and siRNA-LINC0126 groups ($p > 0.05$), Moreover, mRNA and protein expression of CARD11, Ki67, N-cadherin, MMP-9, NF-κBp65, NF-κBp50, E-cad and p53 did not differ between the LINC01260 vector + CARD11 vector and siRNA-LINC01260 + siRNA-CARD11 groups ($p > 0.05$) or between the LINC01260 vector + CARD11 vector and siRNA-LINC01260 + siRNA-CARD11 groups ($p > 0.05$) (Fig 5). These findings reveal that LINC01260 represses CARD11 and inactivates the NF-κB signaling pathway.

Overexpressed LINC01260 or siRNA-CARD11 decreases cell proliferation

The MTT assay was performed to evaluate cell proliferation. The proliferation of U251 glioma cells in each group was accelerated from 24 h, 48 h to 72 h. There was no remarkable difference in proliferation of U251 glioma cells between the blank and NC groups, the LINC01260 vector and siRNA-CARD11 groups, the CARD11 vector and siRNA-LINC01260 groups, or the LINC01260 vector + CARD11 vector and siRNA-LINC01260 + siRNA-CARD11 groups ($p > 0.05$). Compared with the blank and NC groups, the proliferation of U251 glioma cells was markedly decreased in the LINC01260 vector and siRNA-CARD11 groups ($p < 0.05$) and was observably increased in the CARD11 vector and siRNA-LINC01260 groups ($p < 0.05$). However, there was no significant change in the proliferation of U251 glioma cells between

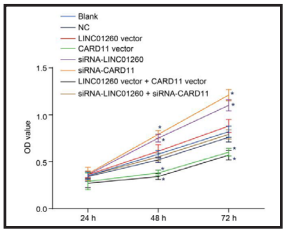

Fig. 6. U251 cell proliferation at 24 h, 48 h and 72 h among eight groups, as determined by the MTT assay. Notes: *, p<0.05, compared with blank and NC groups (n = 3). NC, negative control; LINC01260, non-coding RNA LINC01260; CARD11, caspase recruitment domain family, member 11; OD, optical density.

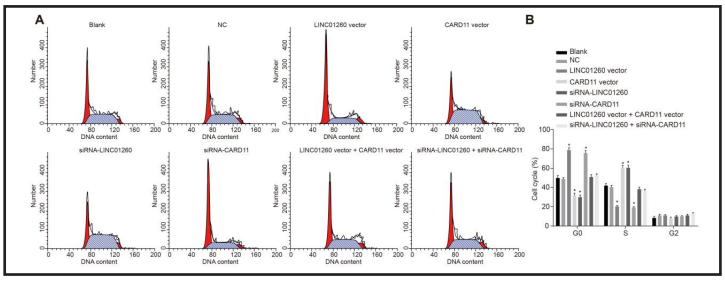

Fig. 7. Changes in U251 glioma cell cycle distribution after transfection among eight groups, as assessed by flow cytometry. Notes: A, Flow cytometry image for the U251 glioma cell cycle distribution after transfection among eight groups. B, Histogram for the cell cycle among the eight groups; *, p<0.05, compared with blank and NC groups (n = 3). NC, negative control; LINC01260, non-coding RNA LINC01260; CARD11, caspase recruitment domain family, member 11.

the LINC01260 vector + CARD11 vector and siRNA-LINC01260 + siRNA-CARD11 groups (p > 0.05) (Fig 6). Therefore, it is suggested that up-regulation of LINC01260 or down-regulation of CARD11 can inhibit glioma cell proliferation.

Overexpressed LINC01260 or siRNA-CARD11 enhances glioma cell cycle and apoptosis

Flow cytometry was used to examine the cell cycle and apoptosis. There was no remarkable difference in cell cycle distribution between the blank and NC groups, the LINC01260 vector and siRNA-CARD11 groups, the CARD11 vector and siRNA-LINC01260 groups, or the LINC01260 vector + CARD11 vector and siRNA-LINC01260 + siRNA-CARD11 groups (p > 0.05). Compared with the blank and NC groups, the number of cells in G1 phase was notable increased, but the number in S and G2 phases was remarkably decreased in the LINC01260 vector and siRNA-CARD11 groups (p < 0.05). The number of cells in G1 phase was significantly reduced but that in S and G2 phase was markedly elevated in the CARD11 vector and siRNA-LINC01260 groups (p < 0.05). Conversely, no substantial change was observed between the LINC01260 vector + CARD11 vector and the siRNA-LINC01260 + siRNA-CARD11 groups (p > 0.05) (Fig 7).

The results of Annexin V/PI double staining revealed no remarkable difference in apoptotic rate between the blank (5.71 ± 0.60)% and NC (5.90 ± 0.60)% groups, the LINC01260 vector (18.05 ± 1.90)% and siRNA-CARD11 (19.00 ± 2.10)% groups, the CARD11 vector (1.05 ± 0.30)% and siRNA-LINC01260 (1.10 ± 0.25)% groups, or the LINC01260 vector + CARD11 vector (6.00 ± 0.80)% and siRNA-LINC01260 + siRNA-CARD11 (5.86 ± 0.70)% groups (all p > 0.05). Compared with the blank and NC groups, the apoptotic rate of U251 glioma cells was substantially elevated in the LINC01260 vector and siRNA-CARD11 groups (p < 0.05) but was strongly reduced in the CARD11 vector and siRNA-LINC01260 groups (p < 0.05). No significant change in the apoptotic rate of U251 glioma cells was observed between the LINC01260 vector + CARD11 vector and siRNA-LINC01260 + siRNA-CARD11 groups (p > 0.05) (Fig 8). These findings indicate that up-regulation of LINC01260 or down-regulation of CARD11 enhances glioma cell apoptosis.

Overexpressed LINC01260 or siRNA-CARD11 inhibits cell migration and invasion

Wound-healing (Fig 9A) and Transwell (Fig 9B) assays were performed to identify cell migration and invasion. No marked difference in migration and invasion of U251

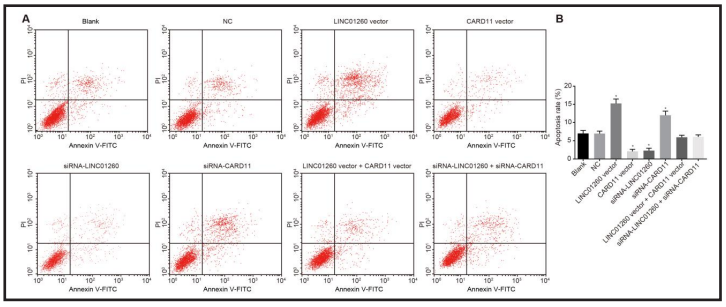

Fig. 8. Flow cytometric detection of U251 glioma cell apoptosis following transfection among eight groups. Notes: A, Flow cytometry image for U251 glioma cell apoptosis following transfection among eight groups. B, Histogram of apoptosis among the eight groups; *, p<0.05, compared with blank and NC groups (n = 3). NC, negative control; LINC01260, non-coding RNA LINC01260; CARD11, caspase recruitment domain family, member 11.

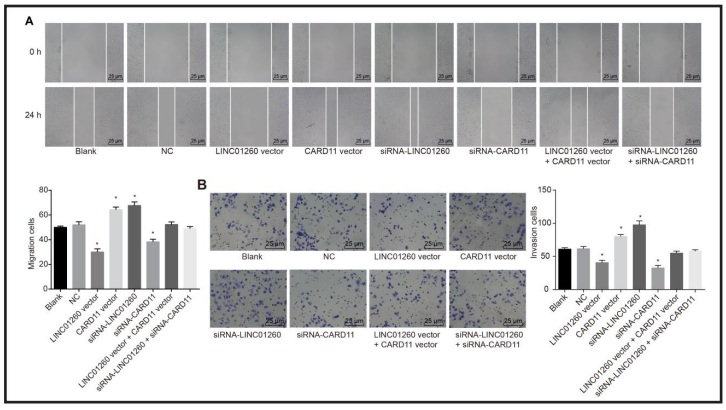

Fig. 9. U251 glioma cell migration and invasion after transfection among eight groups, as confirmed by wound-healing and Transwell assays. Notes: A, Cell migration after transfection among the eight groups, as detected by the wound-healing assay. B, Cell invasion conditions after transfection among the eight groups, as confirmed by the Transwell assay; *, p<0.05, compared with blank and NC groups (n = 3). NC, negative control; LINC01260, non-coding RNA LINC01260; CARD11, caspase recruitment domain family, member 11.

glioma cells between the blank and NC groups, the LINC01260 vector and siRNA-CARD11 groups, the CARD11 vector and siRNA-LINC01260 groups, or the LINC01260 vector + CARD11 vector and siRNA-LINC01260 + siRNA-CARD11 groups ($p > 0.05$) was found. Compared with the blank and NC groups, cell migration and invasion abilities were substantially decreased in the LINC01260 vector and siRNA-CARD11 groups ($p < 0.05$) and elevated in the CARD11 vector and siRNA-LINC01260 groups ($p < 0.05$). There was no significant change in cell migration and invasion between the LINC01260 vector + CARD11 vector and siRNA-LINC01260 + siRNA-CARD11 groups ($p > 0.05$). Taken together, these results reveal that up-regulation of LINC01260 or down-regulation of CARD11 suppresses glioma cell migration and invasion.

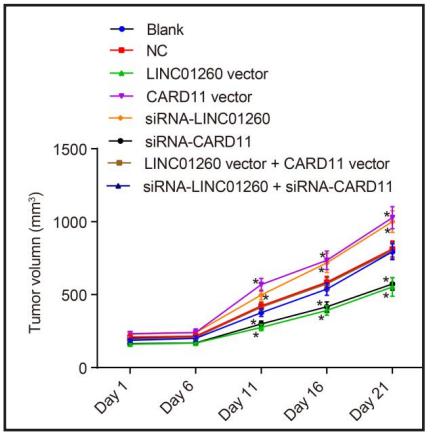

Fig. 10. Growth curves based on changes in tumor volume of nude mice at different time points. Notes: *, p<0.05, compared with blank and NC groups at the same time point (n = 3). NC, negative control; LINC01260, non-coding RNA LINC01260; CARD11, caspase recruitment domain family, member.

Overexpression of LINC01260 or siRNA-CARD11 inhibits tumor growth in nude mice

Xenograft tumors in nude mice were employed to observe tumor growth (Fig 10). Compared with the blank and NC groups, tumor growth was clearly inhibited in the LINC01260 vector and siRNA-CARD11 groups and enhanced in the CARD11

vector and siRNA-LINC01260 groups ($p < 0.05$), though no change was found between the LINC01260 vector + CARD11 vector and siRNA-LINC01260 + siRNA-CARD11 groups ($p > 0.05$). In addition, there was no marked change in tumor growth in the NC group in comparison to the blank group ($p > 0.05$). The results suggest that overexpression of LINC01260 or siRNA-CARD11 represses tumor growth in nude mice.

Discussion

Glioma is an aggressive brain tumor that exhibits high resistance to chemotherapy [20]. The functional effects of lncRNAs have been verified, including their role as key regulators of translational and transcriptional products that influence cellular functions [21-23]. The present study investigated the effects of LINC01260 on the proliferation, migration and invasion of spinal cord glioma cells. We found that overexpression of LINC01260 inhibited spinal cord glioma cell proliferation, migration and invasion by targeting CARD11 via suppression of NF-κB signaling.

The glioma tissues in this study presented decreased expression of LINC01260 but elevated mRNA and protein expression of CARD11 in comparison with adjacent normal tissues. A previous study indicated the potential effects of lncRNAs on the biogenesis, differentiation and development of gliomas, providing an obvious platform for glioma studies [24]. Moreover, lncRNAs might contribute to brain development, and some specific differentially expressed lncRNAs might exert strong effects on the pathogenesis of glioblastoma [25]. Furthermore, specific lncRNAs may serve as tumor inhibitors or oncogenes, which have similar functions [26]. For example, expression of Maternally Expressed Gene 3 (MEG3) is markedly reduced in glioma tissues compared to adjacent normal tissues, and MEG3 was found to enhance apoptosis and impair proliferation of U87 and U251 glioma cells [27], which was consistent with the results of the present study. In addition, it has been reported that up-regulation of the lncRNA HOXA transcript at the distal tip (HOTTIP) ameliorates glioma cell apoptosis and attenuates proliferation [28]. Additionally, CARD11 is predicated to be a target gene of LINC01260 and to be associated with NF-κB pathway regulation. LncRNAs are known to affect epigenetics and to regulate gene expression [29], and novel CARD-containing proteins, including CARD11 and CARD14, modulate activation of the NF-κB pathway [30]. Importantly, somatic gain-of-function (GOF) mutations influencing CARD11 have been observed in various forms of diffuse large B-cell lymphoma, in association with constitutive activation of the NF-κB pathway [31-33]. Taken together, these findings indicate that overexpression of LINC01260 and inhibition of CARD11 can suppress glioma.

Moreover, our study revealed that overexpression of LINC01260 and down-regulation of CARD11 might result in increases in expression of E-cadherin and p53 but reductions in expression of Ki67, N-cadherin, MMP-9, NF-κBp65 and NF-κBp50. E-cadherin is well documented as a tumor suppressor, with reduced expression in various cancer types, and E-cadherin levels in cancer patients are strongly connected to recurrence, metastasis, and prognosis of malignancies [34]. Up-regulation of N-cadherin is considered an important factor for tumor formation during the early stages of progression, and it has been demonstrated that N-cadherin levels are important in glioma, serving as a prognostic indicator for patients with high-grade tumors [35]. In addition, a previous meta-analysis suggested that MMP-9 is strongly associated with poor (5 years) prognosis and that MMP-9 detection in glioma tissue should be considered routine in clinical practice of pathology departments [36]. Moreover, neuronal cell death activated by p53 has been demonstrated in various neurodegenerative diseases; activated p53 has been detected in injured spinal neurons [37], and Ki67 immunohistochemistry is a widely applied marker for tumor proliferation [38]. Together with their associated signaling networks, lncRNAs have emerged as novel players in the regulation and induction of the endothelial-mesenchymal transition (EMT) during metastasis [39, 40]. Moreover, many growth factors, including epidermal growth factor, fibroblast growth factor, vascular endothelial growth factor and related signaling proteins such as

NF-κB, PI3K/Akt, Hedgehog, Wnt and Notch, are involved in triggering and participating in EMT [41]. Furthermore, NF-κB is involved in prostatic disease progression (neoplasic and inflammatory) [42], and it has been shown that the oncogenic risk of constitutive NF-κB activation due to germline CARD11 gain-of-function (GOF) mutations might elevate B-cell malignancy resulting from a larger number of naïve B cells [43]. The NF-κB transcription factor family has great effects on many inflammatory and immune responses, including the response to cancer [44]. Although the specific mechanism of lncRNAs is well understood, most lncRNAs exert their biological function via interaction with other molecules [45], such as microRNAs, other lncRNAs, genomic DNA, and, in particular, proteins involved in vital pathways such as NF-κB signaling [45]. These findings provide evidence that overexpression of LINC01260 and inhibition of CARD11 may inhibit the development of spinal cord glioma via the NF-κB pathway.

Furthermore, the results of this study demonstrate that overexpression of LINC01260 or siRNA-CARD11 might promote apoptosis but repress proliferation and invasion. CARD11 might interact with the pro-apoptotic protein Bcl-10, and CARD11 overexpression may enhance NF-κB activation [46]. In addition, oncogenic mutations in CARD11 are reportedly related to several types of lymphoma progression [31], and CARD11 expression in leukocytes suggests that it might influence immune/inflammatory responses to epithelial ovarian cancer [44]. Thus, we conclude that suppression of CARD11 suppresses proliferation and invasion and facilitates apoptosis of glioma cells via the NF-κB pathway.

Our study demonstrated that overexpression of LINC01260 inhibits spinal cord glioma cell proliferation, migration and invasion by targeting CARD11 via repression of NF-κB signaling. These findings might provide new therapeutic targets for spinal cord glioma. Further work will attempt to address the potential prognostic utility of this biomarker.

Acknowledgements

This work was supported by the Priority Academic Program Development of Jiangsu Higher Education Institutions (PAPD), the 2016 "333 Project" Award of Jiangsu Province, the 2013 "Qinglan Project" of the Young and Middle-aged Academic Leader of Jiangsu College and University, the National Natural Science Foundation of China (81571055, 81400902, 81271225, 31201039, 81171012, and 30950031), the Major Fundamental Research Program of the Natural Science Foundation of the Jiangsu Higher Education Institutions of China (13KJA180001), and grants from the Cultivate National Science Fund for Distinguished Young Scholars of Jiangsu Normal University. We would like express our sincere appreciation to the reviewers for their critical comments on this article.

Disclosure Statement

The authors declare to have no competing interests.

References

1 Yang TQ, Lu XJ, Wu TF, Ding DD, Zhao ZH, Chen GL, Xie XS, Li B, Wei YX, Guo LC, Zhang Y, Huang YL, Zhou YX, Du ZW: MicroRNA-16 inhibits glioma cell growth and invasion through suppression of BCL2 and the nuclear factor-kappaB1/MMP9 signaling pathway. Cancer Sci 2014;105:265-271.

2 Kimura H, Zhang L, Zhao M, Hayashi K, Tsuchiya H, Tomita K, Bouvet M, Wessels J, Hoffman RM: Targeted therapy of spinal cord glioma with a genetically modified Salmonella typhimurium. Cell Prolif 2010;43:41-48.

3 Liu X, Song B, Li S, Wang N, Yang H: Identification and functional analysis of the risk microRNAs associated with cerebral low-grade glioma prognosis. Mol Med Rep 2017;16:1173-1179.

4 Grill J, Kalifa C, Doireau V: Intramedullary spinal cord astrocytomas in children. Pediatr Blood Cancer 2005;45:80.
5 Yu K, Fan J, Ding X, Li C, Wang J, Xiang Y, Wang QS: Association study of a functional copy number variation in the WWOX gene with risk of gliomas among Chinese people. Int J Cancer 2014;135:1687-1691.
6 Milano MT, Johnson MD, Sul J, Mohile NA, Korones DN, Okunieff P, Walter KA: Primary spinal cord glioma: a Surveillance, Epidemiology, and End Results database study. J Neurooncol 2010;98:83-92.
7 Li J, Zhang M, An G, Ma Q: LncRNA TUG1 acts as a tumor suppressor in human glioma by promoting cell apoptosis. Exp Biol Med (Maywood) 2016;241:644-649.
8 Ponting CP, Oliver PL, Reik W: Evolution and functions of long noncoding RNAs. Cell 2009;136:629-641.
9 Bian S, Sun T: Functions of noncoding RNAs in neural development and neurological diseases. Mol Neurobiol 2011;44:359-373.
10 Zhang H, Chen Z, Wang X, Huang Z, He Z, Chen Y: Long non-coding RNA: a new player in cancer. J Hematol Oncol 2013;6:37.
11 Wu C, de Miranda NF, Chen L, Wasik AM, Mansouri L, Jurczak W, Galazka K, Dlugosz-Danecka M, Machaczka M, Zhang H, Peng R, Morin RD, Rosenquist R, Sander B, Pan-Hammarstrom Q: Genetic heterogeneity in primary and relapsed mantle cell lymphomas: Impact of recurrent CARD11 mutations. Oncotarget 2016;7:38180-38190.
12 Tornatore L, Thotakura AK, Bennett J, Moretti M, Franzoso G: The nuclear factor kappa B signaling pathway: integrating metabolism with inflammation. Trends Cell Biol 2012;22:557-566.
13 Jiang L, Lin C, Song L, Wu J, Chen B, Ying Z, Fang L, Yan X, He M, Li J, Li M: MicroRNA-30e* promotes human glioma cell invasiveness in an orthotopic xenotransplantation model by disrupting the NF-kappaB/IkappaBalpha negative feedback loop. J Clin Invest 2012;122:33-47.
14 Li J, Gong LY, Song LB, Jiang LL, Liu LP, Wu J, Yuan J, Cai JC, He M, Wang L, Zeng M, Cheng SY, Li M: Oncoprotein Bmi-1 renders apoptotic resistance to glioma cells through activation of the IKK-nuclear factor-kappaB Pathway. Am J Pathol 2010;176:699-709.
15 Mantovani A: Molecular pathways linking inflammation and cancer. Curr Mol Med 2010;10:369-373.
16 Vivian J, Rao AA, Nothaft FA, Ketchum C, Armstrong J, Novak A, Pfeil J, Narkizian J, Deran AD, Musselman-Brown A, Schmidt H, Amstutz P, Craft B, Goldman M, Rosenbloom K, Cline M, O'Connor B, Hanna M, Birger C, Kent WJ, Patterson DA, Joseph AD, Zhu J, Zaranek S, Getz G, Haussler D, Paten B: Toil enables reproducible, open source, big biomedical data analyses. Nature Biotechnology 2017;35:314-316.
17 Adler P, Kolde R, Kull M, Tkachenko A, Peterson H, Reimand J, Vilo J: Mining for coexpression across hundreds of datasets using novel rank aggregation and visualization methods. Genome Biol 2009;10:R139.
18 Hu R, Sun X: lncRNATargets: A platform for lncRNA target prediction based on nucleic acid thermodynamics. J Bioinform Comput Biol 2016;14:1650016.
19 Wang J, Sun L, Myeroff L, Wang X, Gentry LE, Yang J, Liang J, Zborowska E, Markowitz S, Willson JK, et al.: Demonstration that mutation of the type II transforming growth factor beta receptor inactivates its tumor suppressor activity in replication error-positive colon carcinoma cells. J Biol Chem 1995;270:22044-22049.
20 Jakubowicz-Gil J, Badziul D, Langner E, Wertel I, Zajac A, Rzeski W: Temozolomide and sorafenib as programmed cell death inducers of human glioma cells. Pharmacol Rep 2017;69:779-787.
21 Mercer TR, Qureshi IA, Gokhan S, Dinger ME, Li G, Mattick JS, Mehler MF: Long noncoding RNAs in neuronal-glial fate specification and oligodendrocyte lineage maturation. BMC Neurosci 2010;11:14.
22 Chen LL, Carmichael GG: Decoding the function of nuclear long non-coding RNAs. Curr Opin Cell Biol 2010;22:357-364.
23 Loewer S, Cabili MN, Guttman M, Loh YH, Thomas K, Park IH, Garber M, Curran M, Onder T, Agarwal S, Manos PD, Datta S, Lander ES, Schlaeger TM, Daley GQ, Rinn JL: Large intergenic non-coding RNA-RoR modulates reprogramming of human induced pluripotent stem cells. Nat Genet 2010;42:1113-1117.
24 Zhang X, Sun S, Pu JK, Tsang AC, Lee D, Man VO, Lui WM, Wong ST, Leung GK: Long non-coding RNA expression profiles predict clinical phenotypes in glioma. Neurobiol Dis 2012;48:1-8.
25 Ellis BC, Molloy PL, Graham LD: CRNDE: A Long Non-Coding RNA Involved in CanceR, Neurobiology, and DEvelopment. Front Genet 2012;3:270.
26 Jen J, Tang YA, Lu YH, Lin CC, Lai WW, Wang YC: Oct4 transcriptionally regulates the expression of long non-coding RNAs NEAT1 and MALAT1 to promote lung cancer progression. Mol Cancer 2017;16:104.
27 Wang P, Ren Z, Sun P: Overexpression of the long non-coding RNA MEG3 impairs *in vitro* glioma cell proliferation. J Cell Biochem 2012;113:1868-1874.

28 Xu LM, Chen L, Li F, Zhang R, Li ZY, Chen FF, Jiang XD: Over-expression of the long non-coding RNA HOTTIP inhibits glioma cell growth by BRE. J Exp Clin Cancer Res 2016;35:162.
29 Cao J: The functional role of long non-coding RNAs and epigenetics. Biol Proced Online 2014;16:11.
30 Bertin J, Wang L, Guo Y, Jacobson MD, Poyet JL, Srinivasula SM, Merriam S, DiStefano PS, Alnemri ES: CARD11 and CARD14 are novel caspase recruitment domain (CARD)/membrane-associated guanylate kinase (MAGUK) family members that interact with BCL10 and activate NF-kappa B. J Biol Chem 2001;276:11877-11882.
31 Chan W, Schaffer TB, Pomerantz JL: A quantitative signaling screen identifies CARD11 mutations in the CARD and LATCH domains that induce Bcl10 ubiquitination and human lymphoma cell survival. Mol Cell Biol 2013;33:429-443.
32 Dong G, Chanudet E, Zeng N, Appert A, Chen YW, Au WY, Hamoudi RA, Watkins AJ, Ye H, Liu H, Gao Z, Chuang SS, Srivastava G, Du MQ: A20, ABIN-1/2, and CARD11 mutations and their prognostic value in gastrointestinal diffuse large B-cell lymphoma. Clin Cancer Res 2011;17:1440-1451.
33 Montesinos-Rongen M, Schmitz R, Brunn A, Gesk S, Richter J, Hong K, Wiestler OD, Siebert R, Kuppers R, Deckert M: Mutations of CARD11 but not TNFAIP3 may activate the NF-kappaB pathway in primary CNS lymphoma. Acta Neuropathol 2010;120:529-535.
34 Chung Y, Law S, Kwong DL, Luk JM: Serum soluble E-cadherin is a potential prognostic marker in esophageal squamous cell carcinoma. Dis Esophagus 2011;24:49-55.
35 Asano K, Duntsch CD, Zhou Q, Weimar JD, Bordelon D, Robertson JH, Pourmotabbed T: Correlation of N-cadherin expression in high grade gliomas with tissue invasion. J Neurooncol 2004;70:3-15.
36 Yang X, Lv S, Liu Y, Li D, Shi R, Tang Z, Fan J, Xu Z: The Clinical Utility of Matrix Metalloproteinase 9 in Evaluating Pathological Grade and Prognosis of Glioma Patients: A Meta-Analysis. Mol Neurobiol 2015;52:38-44.
37 Kotipatruni RR, Dasari VR, Veeravalli KK, Dinh DH, Fassett D, Rao JS: p53- and Bax-mediated apoptosis in injured rat spinal cord. Neurochem Res 2011;36:2063-2074.
38 Leonardo E, Volante M, Barbareschi M, Cavazza A, Dei Tos AP, Bussolati G, Papotti M: Cell membrane reactivity of MIB-1 antibody to Ki67 in human tumors: fact or artifact? Appl Immunohistochem Mol Morphol 2007;15:220-223.
39 Xu Q, Deng F, Qin Y, Zhao Z, Wu Z, Xing Z, Ji A, Wang QJ: Long non-coding RNA regulation of epithelial-mesenchymal transition in cancer metastasis. Cell Death Dis 2016;7:e2254.
40 Malek E, Jagannathan S, Driscoll JJ: Correlation of long non-coding RNA expression with metastasis, drug resistance and clinical outcome in cancer. Oncotarget 2014;5:8027-8038.
41 Sanchez-Tillo E, Liu Y, de Barrios O, Siles L, Fanlo L, Cuatrecasas M, Darling DS, Dean DC, Castells A, Postigo A: EMT-activating transcription factors in cancer: beyond EMT and tumor invasiveness. Cell Mol Life Sci 2012;69:3429-3456.
42 Bouraoui Y, Ben Jemaa A, Rodriguez G, Ben Rais N, Fraile B, Paniagua R, Sellemi S, Royuela M, Oueslati R: Profile of NF-kappaBp(65/NFkappaBp50) among prostate specific antigen sera levels in prostatic pathologies. Pathol Biol (Paris) 2012;60:301-305.
43 Snow AL, Xiao W, Stinson JR, Lu W, Chaigne-Delalande B, Zheng L, Pittaluga S, Matthews HF, Schmitz R, Jhavar S, Kuchen S, Kardava L, Wang W, Lamborn IT, Jing H, Raffeld M, Moir S, Fleisher TA, Staudt LM, Su HC, Lenardo MJ: Congenital B cell lymphocytosis explained by novel germline CARD11 mutations. J Exp Med 2012;209:2247-2261.
44 Block MS, Charbonneau B, Vierkant RA, Fogarty Z, Bamlet WR, Pharoah PD, Georgia C-T, for A, Group ACS, Rossing MA, Cramer D, Pearce CL, Schildkraut J, Menon U, Kjaer SK, Levine DA, Gronwald J, Culver HA, Whittemore AS, Karlan BY, Lambrechts D, et al.: Variation in NF-kappaB signaling pathways and survival in invasive epithelial ovarian cancer. Cancer Epidemiol Biomarkers Prev 2014;23:1421-1427.
45 Quinn JJ, Chang HY: Unique features of long non-coding RNA biogenesis and function. Nat Rev Genet 2016;17:47-62.
46 Gaide O, Martinon F, Micheau O, Bonnet D, Thome M, Tschopp J: Carma1, a CARD-containing binding partner of Bcl10, induces Bcl10 phosphorylation and NF-kappaB activation. FEBS Lett 2001;496:121-127.